

$$\omega_p = \sqrt{\frac{ne^2}{m\epsilon_0}}, \quad (3.4)$$

where e and m denote the charge and mass of an electron, respectively, and ϵ_0 denotes the permittivity of free space.

3.3.3 Magnetic Field (MGF) instrument

The MGF instrument measures magnetic field variations ranging from DC frequencies to 100 Hz. The MGF data clarifies the generation mechanism of the field aligned current that connects the magnetosphere and ionosphere, and the role of this current in auroral particle acceleration. The sampling frequency depends on the observation mode, being 32 Hz, 8 Hz, and 2 Hz in modes Bit-H, Bit-M, and Bit-L, respectively. When the ELF receiver detected natural plasma waves, the ion cyclotron frequencies were computed from the magnetic field measurements collected by the MGF instrument. Since the ELF receiver is nonfunctional in the Bit-M and Bit-L modes of the MGF instrument, we use only the 32 Hz sampling data observed in Bit-H mode. The ion cyclotron angular frequency (Ω_i) is then calculated from the intensity of the background geomagnetic field $|\mathbf{B}|$ as follows:

$$\Omega_i = \frac{q_i |\mathbf{B}|}{m_i}, \quad (3.5)$$

where q_i and m_i denote the charge and mass of ion species i , respectively. The derivations are detailed in Appendix A.

3.4 Usage of ELF data

3.4.1 Absolute value calibration

Apart from the PFX data, the waveform data accumulated in VLF observations are stored as one-word (8 bit) PCM data. The PFX data (with 12 bit resolution) are compressed into 1 word (8 bit) data. The output amplitudes V_{out} of the PFX and the ELF receiver are computed by substituting the stored digital value D_{out} into the following equations:

$$V_{\text{out}} = \frac{\sqrt{2}}{2^{n-1}} \cdot D_{\text{out}}, \quad (3.6)$$

$$-2^{(n-1)} \leq D_{\text{out}} \leq 2^{(n-1)} - 1, \quad (3.7)$$

where the parameter n indicates the resolution (12 and 8 for PFX and ELF data, respectively).

Note that the data output from each subsystem are amplified depending on the observation environment and must be corrected prior to analysis. Each subsystem was equipped with wide dynamic range amplifier (WIDA) IC stacks, and the receiver gains were automatically altered every 0.5 seconds. A signal passing through a WIDA IC is amplified 25 dB. The number of executing WIDA ICs is indicated by the recorded WIDA statuses W_s . The output amplitude of the DPU COM (V_{DPU}) is then obtained by inserting W_s into the following equation:

$$V_{\text{DPU}} = V_{\text{out}} - 25 \cdot W_s. \quad (3.8)$$

To derive the absolute intensity of an observed electric and magnetic field, we have to consider the effective length of antennas. For a pair of wire antennae that observe an electric field below 160 (80) Hz in ELF-NARROW (ELF-WIDE) mode, we use half of the antenna length as the effective length h_{eff} (equation (3.9)).

$$h_{\text{eff}} = \frac{2 \times 30}{2} = 30 \text{ m}. \quad (3.9)$$

For the three axes' search coils that observe the magnetic field, the effective length l_{eff} changes depending on the frequency f as follows:

$$l_{\text{eff}} = \begin{cases} 10^{(\log f - 1.0) \times 0.8921 - 1.6999} & (f < 164.4 \text{ Hz}) \\ 0.243 & (164.4 \text{ Hz} < f \leq 800.0 \text{ Hz}) \\ 10^{(\log f - 3.0) \times 1.0588 - 0.9208} & (800.0 \text{ Hz} < f \leq 7407.0 \text{ Hz}) \\ 10 & (7407.0 \text{ Hz} < f \leq 10000.0 \text{ Hz}) \\ 10^{(4.2504 - \log f) \times 0.88591 - 0.22185} & (f > 10000.0 \text{ Hz}) \end{cases} \quad (3.10)$$

Considering the effective length of the antenna, the impedance of the antenna, and the gains of the preamplifier and amplifier inside DPU COM, calibrated electric field intensity E and magnetic field intensity B are represented in the following

equations:

$$V_{\text{E-DPU}} = E \cdot h_{\text{eff}} \cdot \left| \frac{Z_{\text{in}}}{Z_{\text{WAT}} + Z_{\text{in}}} \right| \cdot G_{\text{E-pre}} \cdot G_{\text{E-DPU}}, \quad (3.11)$$

$$V_{\text{B-DPU}} = \frac{Z_0 \cdot B}{\mu_0} \cdot l_{\text{eff}} \cdot G_{\text{B-DPU}}, \quad (3.12)$$

where Z_{in} and Z_{WAT} denote the impedance of the preamplifier and wire antennas, respectively. $G_{\text{E-pre}}$, $G_{\text{E-DPU}}$, and $G_{\text{B-DPU}}$ denote the gains from the preamplifier, the DPU COM for the wire antennas, and the DPU COM for the search coils, respectively. Z_0 and μ_0 denote the impedance and permeability of free space, respectively. These parameters are as follows:

$$Z_{\text{in}} = \frac{1}{j\omega \cdot C_{\text{in}}}, \quad (3.13)$$

$$Z_{\text{WAT}} = \frac{1}{\frac{1}{R_s} + j\omega \cdot C_s}, \quad (3.14)$$

$$G_{\text{E-pre}} = -2.1 \sim -2.2 \text{ dB}, \quad (3.15)$$

$$G_{\text{E-DPU}} = 20 \text{ dB}, \quad (3.16)$$

$$G_{\text{B-DPU}} = 25 \text{ dB (for three axes search coils)}, \quad (3.17)$$

$$G_{\text{B-DPU}} = 25 \text{ dB (for loop antennas)}, \quad (3.18)$$

$$Z_0 = 377 \Omega, \quad (3.19)$$

$$\mu_0 = 4\pi \times 10^{-7} \text{ H/m}, \quad (3.20)$$

where R_s and C_s denote the resistance and capacitance of the antenna impedance, respectively, i.e., $R_s = 500 \text{ k}\Omega$ and $C_s = 250 \text{ pF}$. C_{in} denotes the capacitance of the impedance of the preamplifier, i.e., $C_s = 100 \text{ pF}$.

3.4.2 Removing spinning motion effect

As described in the previous section, the Akebono satellite spins with a period of nearly 8 seconds. Since the onboard antennas also rotate by spin motion, the observed waveforms and spectra must be corrected for the spinning motion effect. Such an effect inhibits precise analysis when each axis of the waveform data is independently analyzed. Here, we define the nonspinning coordinate system (X_0 , Y_0 , Z_0) as the direction of Z_0 aligned with Z in the satellite coordinate system. The spin axis is always parallel to the sunward direction, and the satellite rotates clockwise (See Figure 3.4). We can regard the rotation axis as fixed and the

satellite as rotating in the X–Y plane, because the spinning axis is accurate to within 3 degrees. The spin phase of the satellite, which indicates the rotation angle from the reference point in the X–Y plane, is yet to be determined.

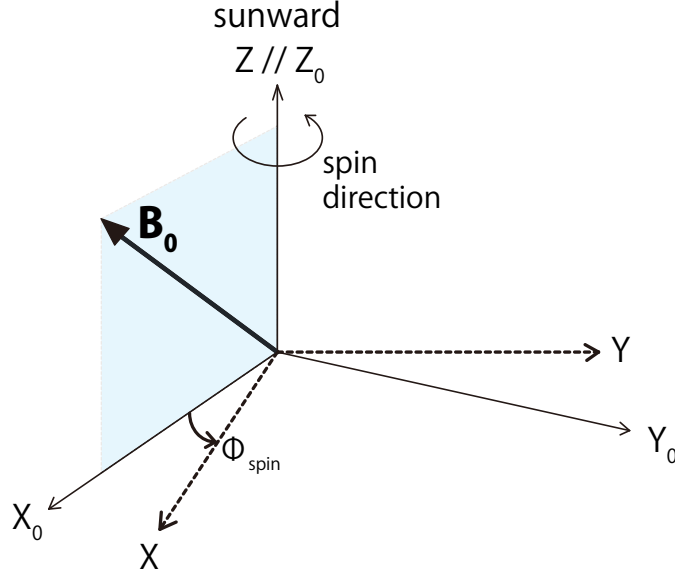


FIGURE 3.4: Relation between the satellite coordinate system (X, Y, Z) and the nonspinning coordinate system (X₀, Y₀, Z₀).

Assuming that the geomagnetic field remains stable throughout one period of the satellite spin, the spin phase of the satellite can be determined from the DC magnetic field measurements obtained by the MGF instrument. An example of such measurements during a 30 seconds interval is shown in Figure 3.5. In Figure 3.5, the red, green, and blue lines indicate the intensities of the X, Y, and Z components of the observed DC magnetic field, respectively, in satellite coordinates (before removing the spinning motion). As evident in this figure, the spin motion alters the intensities of the X and Y components. The Z component is almost stable because the spinning axis is almost aligned with the Z axis. Here the intensity of the geomagnetic field observed in the satellite coordinate system is denoted (B_{0X} , B_{0Y} , B_{0Z}). We also define the spin phase $\phi_{\text{spin}} = 0$ under the conditions $B_{0X} = \text{Maximum}$ and $B_{0Y} = 0$. The spin phase is then given as follows:

$$\phi_{\text{spin}} = \arg(B_{0X} - jB_{0Y}). \quad (3.21)$$

The nonspinning coordinate system (X₀, Y₀, Z₀) is obtained by expressing the coordinate transformation as a function of the calculated spin phase ϕ_{spin} . The